Article

Not peer-reviewed version

Transcriptomic Profiling Identifies a Subset of Renal Tumours with Overlapping Features of Clear Cell Papillary Renal Cell Tumour and Renal Cell Carcinoma with Fibromyomatous Stroma

Rasmus Jakobsson , Martin Lindström , Yvonne Arvidsson , Iva Johansson , Jonas A. Nilsson , Niels Marcussen , Joakim Karlsson † , Martin E. Johansson *,†

Posted Date: 15 June 2026

doi: 10.20944/preprints202606.1140.v1

Keywords: renal cell carcinoma; clear cell papillary renal cell tumour; renal cell carcinoma with fibromyomatous stroma

 doi:10.20944/preprints202606.1140.v1

Article

Transcriptomic Profiling Identifies a Subset of Renal Tumours with Overlapping Features of Clear Cell Papillary Renal Cell Tumour and Renal Cell Carcinoma with Fibromyomatous Stroma

Rasmus Jakobsson [1,2,3], Martin Lindström [4,5], Yvonne Arvidsson [3,6], Iva Johansson [6], Jonas A. Nilsson [3,7], Niels Marcussen [8,9], Joakim Karlsson [3,7,†] and Martin E. Johansson [1,3,6,*,†]

[1] Department of Laboratory Medicine, Institute of Biomedicine, Sahlgrenska Academy, University of Gothenburg, Sweden
[2] Department of Surgery and Urology, Skaraborg Hospital, Skövde, Sweden
[3] Sahlgrenska Center for Cancer Research, University of Gothenburg, Sahlgrenska Academy, Gothenburg, Sweden
[4] Department of Translational Medicine, Lund University, Malmö, Sweden
[5] Department of Clinical Pathology, Laboratory Medicine Skåne, Malmö, Sweden
[6] Department of Clinical Pathology, Sahlgrenska University Hospital, Gothenburg, Sweden
[7] Department of Surgery, Institute of Clinical Sciences, The Sahlgrenska Academy, University of Gothenburg, Gothenburg, Sweden
[8] Department of Pathology, University Hospital of Southern Denmark, Aabenraa, Denmark
[9] Institute of Regional Health Research, University of Southern Denmark, Denmark
* Correspondence: martin.e.johansson@gu.se
† These authors contributed equally to this work.

Abstract

Background: Renal cell carcinomas (RCC) represent neoplasms with variable biological behaviour. Some remain difficult to classify within the current diagnostic framework. Clear cell papillary renal cell tumour (CCPRCT) is now recognized as an indolent entity, whereas renal cell carcinoma with fibromyomatous stroma (RCCFMS) remains a provisional subtype with partially overlapping morphological features. **Methods**: We analysed a multifocal RCC with clear cell morphology and prominent fibromyomatous stroma using whole-genome and RNA sequencing. The molecular profile was compared with the Cancer Genome Atlas (TCGA) pan-cancer dataset including 885 RCC cases. Histological re-evaluation of 10 identified similar cases was performed. Transcriptional data was mined for potential markers which were validated in an independent cohort. **Results**: The ten TCGA cases with similar transcriptomic features were characterized by diploid genomes, absence of recurrent chromosomal alterations and lack of *VHL* gene mutations. Reduced *VHL* mRNA expression was observed, with increased methylation at selected CpG sites consistent with possible epigenetic down-regulation. Histological re-evaluation by three urological pathologists identified diagnostic variability. Differential expression analysis highlighted cytokeratin 17 (KRT17) and collagen 17A1 (COL17A1) as candidate markers. Immunohistochemical evaluation in a small (n = 6) independent cohort of CCPRCT demonstrated expression of both markers, whereas tissue microarrays of 257 clear cell and 68 papillary RCC cases were found to be negative. **Conclusions**: These findings suggest that a subset of renal tumours with overlapping morphological features of CCPRCT and RCCFMS may share common molecular characteristics. These observations are exploratory and hypothesis-generating, and further studies in larger, well characterized cohorts are required to clarify the biological and diagnostic significance of this subgroup.

 doi:10.20944/preprints202606.1140.v1

Keywords: renal cell carcinoma; clear cell papillary renal cell tumour; renal cell carcinoma with fibromyomatous stroma

1. Introduction

The formalized histological classification of renal cell carcinoma (RCC) into distinct kidney tumour categories is relatively recent, in contrast to many other forms of cancer [1]. Clear cell (CCRCC), papillary (PRCC) and chromophobe (CHRCC) renal cell carcinoma constitute the major RCC subtypes. However, the increasing application of molecular profiling has led to the recognition of additional entities, now reflected in the 2022 World Health Organization (WHO) classification, where 21 distinct RCC subtypes are defined [2,3]. While this expanded framework has improved diagnostic precision, it has also highlighted challenges in classifying rare or borderline tumours, particularly when diagnostic criteria overlap or remain incompletely defined [4]. This is a significant challenge for diagnosis of renal cell carcinomas and tumours with clear cell histology, known for histological diversity, both within and between cases.

Clear cell papillary renal cell tumour (CCPRCT) and renal cell carcinoma with fibromyomatous stroma (RCCFMS) represent two such diagnostic examples, sharing morphological and immunohistochemical characteristics while differing in classification status and molecular definition.

CCPRCT is a relatively recently defined entity that was included in the WHO Classification in 2016 [5]. In the most recent WHO edition from 2022, it was reclassified and renamed to clear cell papillary renal cell *tumour* due to indolent clinical behaviour [2,3]. It is characterized by clear cell histology and low grade nuclei with at least focal, apically linearized nuclear position in the cells and a diffuse, so-called cup-shaped distribution of carbonic anhydrase 9 (CAIX) expression [2].

Another renal tumour of similar histology was initially described by Michal et al. [6]. This was named renal angiomyomatous tumour (RAT) and was characterized by clear cell morphology and a more distinct fibroleiomyomatous stromal component than CCPRCT [7,8]. The similarities to CCPRCT led to further studies, and the ensuing debate and analyses resulted in the appreciation that CCPRCT and RAT probably represent the same tumour entity, but with variable morphological features [5].

An additional renal tumour with clear cell morphology, debated as a potential single entity, is renal cell carcinoma with (angio)leiomyomatous stroma, most commonly known as RCC with fibromyomatous stroma (RCCFMS) [9]. The tumour displays clear cell morphology with a prominent, dense spindle-cell stroma resembling fibroblasts and/or smooth muscle cells. It is currently regarded as a provisional entity and is characterized by diffuse CK7 expression and cup-shaped CAIX positivity [2]. By analysing a series of 18 cases, Shah et al. demonstrated that this category was characterized by somatic mutations in genes implicated in activation of the mTOR signalling cascade: *TSC1*, *TSC2*, *MTORC1* or in the *ELOC* gene. The *ELOC* gene codes for Elongin C, which is a component of the E3 ubiquitin ligase complex of the von Hippel-Lindau disease (VHL) tumour-suppressor complex and has recently been added to the molecularly defined category in the 2022 WHO classification. The *VHL* gene was found to be structurally intact in RCCFMS, however [10]. Clinically RCCFMS typically associated with indolent behaviour. It is still classified as a low grade malignant renal neoplasm due to occasional reports on metastasis however, most often in the context of tuberous sclerosis syndrome [11]. Other reports may also represent tumours within the broader fibromyomatous spectrum, including ELOC-mutated RCC [12].

The distinction between CCPRCT and RCCFMS in routine practice relies primarily on morphological criteria including nuclear positioning and the extent and composition of stromal elements. [13,14]. However, these features may overlap, and stromal components are not entirely specific, as similar findings can be observed in other RCC subtypes. Alterations in *TSC1*, *TSC2*, and *MTORC1* in RCCFMS are regarded as bona fide driver events, leading to constitutive mTOR activation. The morphologic spectrum most probably encompasses molecularly heterogeneous subgroups, however.

 doi:10.20944/preprints202606.1140.v1

The Cancer Genome Atlas (TCGA) data set comprises an exhaustive molecular analysis of 33 major tumour types, including the three main RCC groups CCRCC, PRCC and chromophobe RCC (CHRCC) [15–17]. The large number of molecularly defined cases makes it a valuable source for taxonomic studies. It has become recognized that the TCGA data may contain less common entities previously attributed to the three major RCC types, where reclassification is warranted [18].

To explore these lesser-studied clear cell entities and their potential relationships, we tested a concept of index-case driven exploratory analysis where we analysed a case fulfilling the histological criteria of an RCCFMS by whole-genome and transcriptomic profiling. We then performed an unbiased exploratory comparison with TCGA data to identify tumours with similar molecular characteristics. Through this approach, we found data suggesting that a subset of renal tumours with fibromyomatous stroma shares some molecular and immunohistochemical features with CCPRCT and identified candidate markers that may aid in their recognition.

2. Materials and Methods

2.1. Case selection

We identified a 50-year-old male patient with hypertension who was incidentally diagnosed with multiple tumours bilaterally in the kidneys, with a largest tumour diameter of 35 mm. Biopsies had been obtained from some of the tumours, as part of the diagnostic work-up. However, morphology and IHC results were not typical for CCRCC. First, the cup-shaped distribution of the CAIX signal was regarded as a problematic diagnostic feature indicating CCPRCT. On the other hand, no apical positioning of the nuclei could be discovered in the limited material available for evaluation precluding unequivocal benign diagnosis. The patient underwent resection of the tumours in the left kidney. With additional material available for evaluation, the tumour was considered to exhibit morphological features of RCCFMS, with CCPRCT representing the closest established subtype. We obtained consent from the patient and approval from the Regional Ethical Review Board of Gothenburg for the use of clinical materials for research purposes including genetic analysis (Dnr: 2019-00905).

2.2. Immunohistochemistry

Tissue from two tumours was formalin-fixed, paraffin-embedded and subjected to antigen retrieval using EnVision FLEX Target Retrieval Solution (high pH) (Dako PT-Link, Agilent Technologies, Santa Clara, CA, US). Immunohistochemical staining was performed in a Dako Autostainer Link using EnVision FLEX according to the manufacturer's instructions (DakoCytomation, Agilent Technologies, Santa Clara, CA, US). Histopathological evaluation was performed using haematoxylin and eosin (H&E)—stained sections and immunohistochemical (IHC) staining for CAIX, cytokeratin 7 (CK7/KRT7), cluster of differentiation 10 (CD10), vimentin, epithelial antibody cocktail 1-3 (AE1-3), epithelial membrane antigen (EMA) and E-cadherin (ECAD). IHC staining was performed using antibodies against collagen Type XVII Alpha 1 Chain (COL17A1, 1:250, no. HPA043673, Atlas Antibodies), cytokeratin 17 (CK17/KRT17, ready to use, no. IR620, Agilent), phospho-mechanistic Target Of Rapamycin Kinase (p-mTOR, 1:25, no. 2976, Cell signalling technology), phospho-S6 Kinase 1(pS6K1, 1:500, no. ab60948, Abcam), VHL (1:1000, no. sc-135657, Santa Cruz Biotechnology) and Tuberous Sclerosis Complex 2 (TSC2, 1:100, no. HPA030409, Atlas Antibodies). More information regarding the antibodies and staining patterns is provided in Supplementary Table S1. The biopsies were reviewed by a board- certified surgical pathologist (MJ).

2.3. Whole genome sequencing (WGS) and RNA sequencing

DNA and RNA were isolated from snap-frozen biopsies from two tumours in the left kidney using the allprep DNA/RNA Mini Kit (Qiagen, Hilden, Germany) according to the manufacturer's protocol. Blood was collected from the patient and DNA was extracted using the DNeasy Blood &

 doi:10.20944/preprints202606.1140.v1

Tissue Kit (Qiagen, Hilden, Germany) and used as the normal tissue. WGS libraries were constructed from the two tumours using the TruSeq PCR free kit (Illumina, San Diego, CA) and sequenced on an Illumina Novaseq 6000 using 150 bp paired-end reads to an average depth of 893 million reads (average coverage: 75X). Transcriptome libraries were constructed from the two tumours using the TruSeq Stranded Total RNA Sample Preparation Kit with Ribo-Zero Gold (Illumina, San Diego, CA) and sequenced on a Nextseq500 using 2 × 75 bp reads to an average depth of 44 million reads. WGS and RNA sequencing were performed at the Genomics Core Facility at the Sahlgrenska Academy, University of Gothenburg.

2.4. RNA-seq processing and normalization

Raw RNA-seq reads were aligned to the UCSC hg19 human genome assembly, excluding alternative haplotype regions, with hisat 0.1.6-beta (parameters: *--no-mixed --no-discordant --no-unal --known-splicesite-infile*) and converted to BAM format using samtools (v. 0.1.19) [19]. RNA-seq data from TCGA for 9,583 tumours from 32 cancer types were downloaded from the cgHub repository on December 18, 2015 and aligned in the same manner. Gene read counts were derived using htseq-count (parameters: *-m intersection-strict -s no*) [20]. For TCGA data, reads per kilobase per million (RPKM) normalized values were calculated, considering the maximum mature transcript length of each gene and using robust size factors as previously described for the DESeq method. Reads from our samples were normalized using the same method, except that standard read- depth based size factors were used for RPKM normalization.

2.5. Gene expression-based classification

To classify a sample using a *k*-nearest neighbour approach, Spearman correlation coefficients with respect to all coding genes were first calculated between the sample of interest and all samples in the TCGA pan-cancer data-set (*cor.test* in R, with the parameter *method= "spearman"*). A prediction was then made using the majority vote of the top *k* most strongly correlated samples. In the case of ties, the value of *k* decreased by one until a majority vote was achieved. A value of $k = 6$ was used, as previously found to be optimal using leave-one-out cross-validation [21]. For analysis with *t*-distributed stochastic neighbour embedding (*t*-SNE), $\log_2$-transformed (pseudo count of 1 added) expression values of all coding genes were used as inputs for the *Rtsne* function from the "Rtsne" R package (v. 0.15) [22].

2.6. Differential expression and gene set enrichment analysis

Wilcoxon rank-sum tests were used to compare the differential expression between primary case samples or similar RCC samples identified in TCGA and the remaining TCGA CCRCC (KIRC) and PRCC (KIRP) samples (*wilcox.test* in R). Adjusted *p*-values (Benjamini-Hochberg correction) <0.1 were considered significant. Log_2 fold changes were calculated as $\log_2$([mean group A + 1] /[mean group B + 1]). To determine genes over/under expressed, the intersect of genes significant and with the same direction of fold change were considered. For comparative pathway analysis, single sample gene set enrichment analysis was performed using the GSVA R package (v. 1.36.3), with the function *gsva* (*method="ssgsea"*, *kcdf="Poisson"*) and Hallmark pathways obtained from MSigDB (*h.all.v7.1.symbols.gmt*) [23]. Differences in normalized enrichment scores across the sample groups of interest were assessed using two-tailed *t*-tests (*t.test* in R), and the resulting *p*-values were adjusted using the Benjamini-Hochberg correction. A False Discovery Rate (FDR-values) <0.05 was considered significant. Gene set enrichment among genes that differed in expression between the two main case tumours was assessed based on $\log_2$ fold changes using the fgsea R package (v. 1.12.0) with the same set of reference pathways (parameters: *minSize=0*, *maxSize=10000*, *nperm=*10^7) [24].

 doi:10.20944/preprints202606.1140.v1

2.7. DNA-seq processing

Raw WGS reads were aligned to the 1000 genomes version of the GRCh37 human reference genome (human_g1k_v37_decoy.fasta), with decoy sequences included, using bwa (v. 0.7.17-r1188; parameters: *mem -t 40 -M -R*) [25]. Samples sequenced across multiple lanes were merged using SAMtools. Duplicate reads were marked using GATK (v. 4.1.3.0) module MarkDuplicates [26]. Base quality scores were recalibrated using the GATK commands BaseRecalibrator and ApplyBQSR in two passes, with the same reference genome used for alignment and with population variant resources obtained from the GATK resource bundle (*dbSNP_138.b37.vcf,1000G_phase1.indels.b37.vcf,Mills_and_1000G_gold_standard.indels.b37.vcf*).

2.8. DNA copy number analysis

Matched tumour and normal WGS BAM files were analysed using CNVkit (v. 0.9.6) using the *batch* command, with the parameters *-m --male-reference* and segmented using the CNVkit *export seg* command.

2.9. Mutation calling

Variant calling using WGS of paired tumour and normal samples was performed with Mutect 2 (GATK v. 4.1.3.0), with the following parameters: *--genotype-germline-sites true*, *--af-of-alleles-not-in-resource 0.0000025*, *--disable-read-filter MateOnSameContigOrNoMappedMateReadFilter*, *--germline-resource* [27]. The gnomAD database was used as a germline resource, as provided in the GATK resource bundle (*af-only-gnomad.raw.sites.b37.vcf*) [28]. The quality of the resulting raw variant calls was assessed with FilterMutectCalls (GATK), using the same reference genome as for alignment. Further annotation was performed using maftools (v. 1.6.17), which uses VEP (v. 98.2), using a version of the ExAC germline variant database with TCGA samples excluded (*ftp://ftp.broadinstitute.org:/pub/ExAC_release/release0.3.1/subsets/ExAC_nonTCGA.r0.3.1.sites.vep.vcf.gz*). The following variants were then removed: population frequency >= 0.001 in gnomAD or ExAC, those present in either the dbSNP or ESP databases but not COSMIC, and those not labelled as PASS by FilterMutectCalls. Prediction of impact for protein sequence variant queries was performed using PolyPhen and SIFT [29,30].

2.10. Analysis of data from the TCGA database

A complete description of the workflow in establishing the TCGA RCC database including tumour identification, sequencing procedures and methylation arrays, has previously been described [31]. In addition to sequencing data, diagnostic H&E slides, clinical records and pathology reports were available from the National Cancer Institute Genome Data Commons (https://gds.cancer.gov/). An easy access overview of histology and pathology reports can also be found in Emory University, Atlanta, U.S. (https://cancer.digitalslidearchive.org) [32]. Three urological pathologists from different universities independently evaluated the identified similar cases (ML, NM, MJ).

2.11. Verification of marker utility

To evaluate the utility of the potential markers KRT17 and COL17A1 for identifying CCPRCT and RCCFMS we stained tissue microarrays (TMA) of CCRCC (n=257 cases) and PRCC (n=68 cases). This as negative verification of the markers. The TMAs were constructed using two representative punch biopsies from surgically resected RCC tumours at a single centre (Malmö University Hospital, Malmö, Sweden). For positive verification, tissue from the index case was used as well as whole tissue sections from five consecutive recently diagnosed CCPRCT cases. Histological evaluation was performed by three independent assessors (MJ, RJ and ML).

 doi:10.20944/preprints202606.1140.v1

2.12. Histological assessment of 10 identified similar tumours from the TCGA data repository

Digitalized histological images from the similar cases identified from the TCGA data sets were downloaded and independently diagnosed by three pathologists specialized in urological pathology working at three university hospitals. Diagnostic criteria were derived from the 2022 edition of the WHO manual.

3. Results

3.1. Histopathological evaluation and marker assessment of the index case

Standard histopathological analysis using H&E staining was performed on four excised tumours from the left kidney of the patient. Microscopically clear or slightly eosinophilic cells were arranged in branching papillary and tubular patterns separated by a focally prominent dense fibromuscular stroma. The nuclei of the tumour cells were mainly localized basally. No areas of apically localized nuclei were present. IHC revealed diffuse CK7 positivity and basolateral ("cup-shaped") CAIX positivity. Diffuse CD10 positivity was also noted (Figure 1A–D). The tumours were considered to show morphological features of RCCFMS, with CCPRCT as the closest differential diagnosis. Additional clinically relevant markers were also tested (Supplementary Table S1).

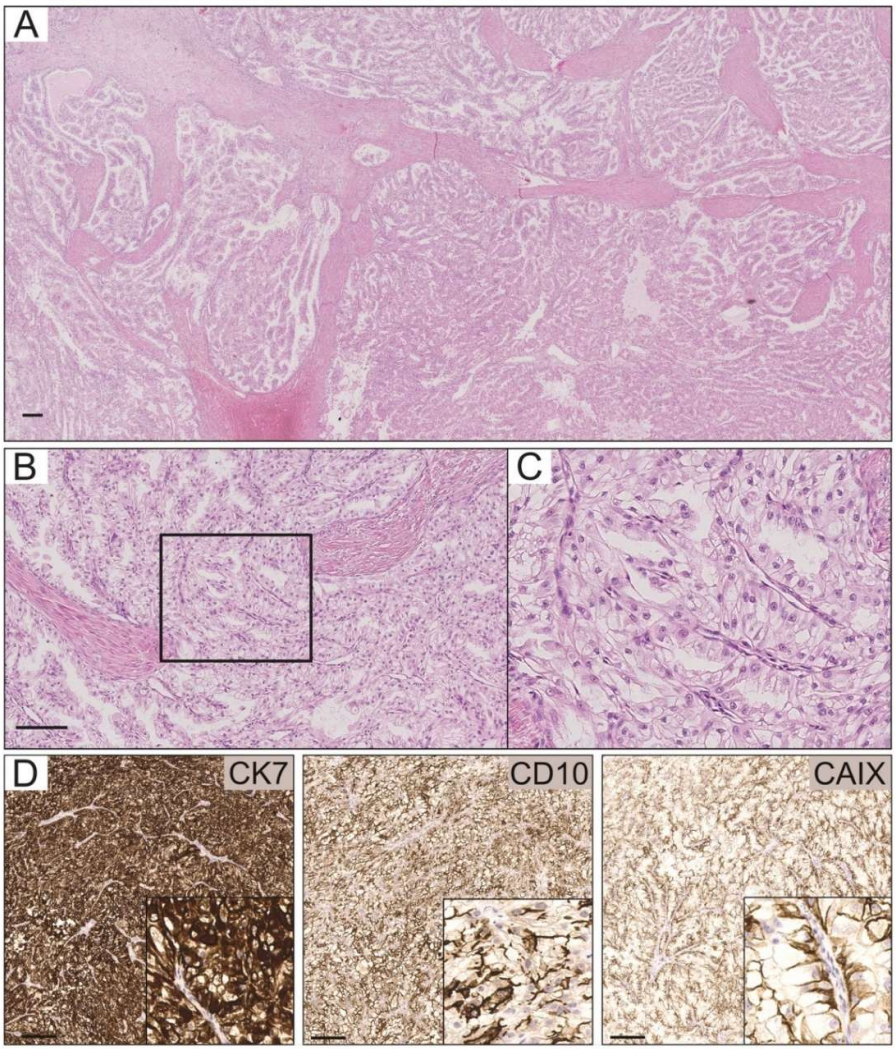

Figure 1. Histological features of the index case. (**A**) Overview of the histology showing the dense fibromatous strands separating the clear cell tumour component. The tumour cells are arranged in both papillary and

 doi:10.20944/preprints202606.1140.v1

tubular/acinar patterns. (**B** and **C**) Higher magnification, showing details of the histology and mainly basally oriented nuclei. (**D**) Cytokeratin 7 (KRT7/CK7) with diffuse, high expression in the tumour component. Cluster of differentiation 10 (CD10) also with diffuse, high expression. Carbonic anhydrase IX (CAIX) with basolateral (cup-shaped) appearance. Scale bars = 200 µm. *HE*: Haematoxylin/Eosin staining.

3.2. Expression analysis and identification of similar tumours in the TCGA data set

Fresh frozen samples from two of the resected tumours, designated T3 and T4, were subjected to WGS to differentiate sub-clonal variations. The tumours were compared to 885 RCC tumours from the TCGA database (530 CCRCC (KIRC), 289 PRCC (KIRP), 66 CHRCC (KICH)). Unsupervised *t*-SNE analysis of RNA-seq data revealed a transcriptomic world map of the 32 available cancer types in TCGA (Figure 2A). T3 and T4 were separately analysed for similarities among RCC tumours. This revealed that the case tumours clustered together with a specific subset of TCGA RCC tumours and formed a distinct separate cluster (Figure 2B). The unique identification numbers are shown in Supplementary Table S4. When T3 and T4 were included in the same analysis, the distance to other tumours expanded owing to the resemblances between the two patient samples. However, clustering remained evident.

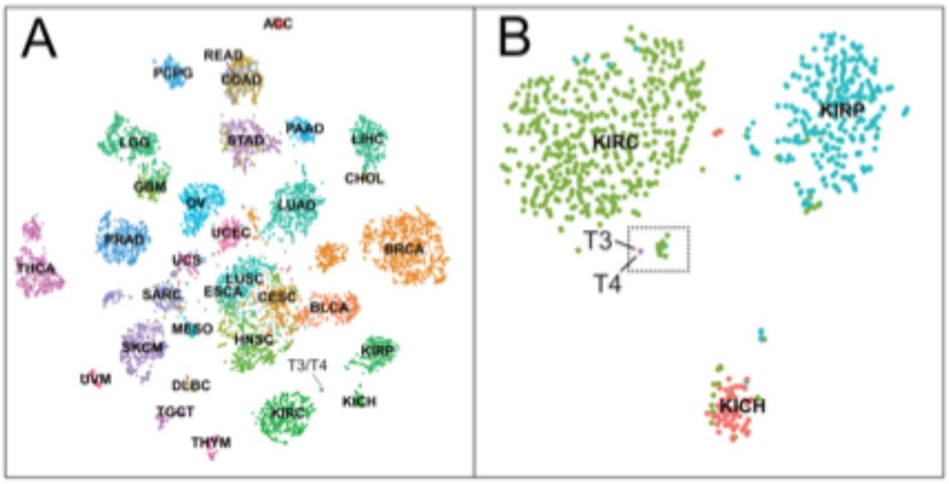

Figure 2. Unsupervised *t*-SNE analyses in two dimensions of RNA-seq data from the index case annotated T3/T4 to the The Cancer Genome Atlas (TCGA). (A) Comparative analysis using the entire TCGA dataset of 32 cancer types (9583 cases). Samples are coloured according to known cancer type and form clusters in the *t*-SNE space. (B) Exploration of the TCGA RCC samples only relative to the index-case tumours. A distinct subcluster with 10 similar RCC patients adjacent to tumour samples T3/T4 was noted. *RCC*: Renal cell carcinoma, *KIRC*: Clear cell RCC, *KIRP*: Papillary RCC, *KICH*: Chromophobe RCC. See Table S6 for complete abbreviation list from TCGA.
.

3.3. Copy Number Profiles and VHL expression

Somatic copy number profiles showed largely diploid genomes in both the index case tumours and the ten most similar TCGA tumours, further supporting their similarity. Sub-clonal variations in T4 included gain of chromosome 12 and loss of chromosome 13. Chromosome 3p was preserved in all 10 similar and the index case tumours (Figure 3A). No genomic alterations in *VHL* were detected in T3 or T4. When analysing the 10 similar cases, only one harboured a genetic mutation in *VHL*. Expression analysis of *VHL* showed significantly lower expression in the index case and in the 10 similar (Figure 3B). In addition, in the sub-cluster, the degree of methylation was generally low, except for the *VHL* gene, where methylation levels were higher in the group. Specifically, several important CpG probes exhibited significantly increased methylation indicative of epigenetic silencing, including cg13672843 (Figure 3C,D). Increased methylation of probe cg13672843 resulted

 doi:10.20944/preprints202606.1140.v1

in lower *VHL* expression in the sub-cluster compared to other RCC tumours (Figure 3E). IHC of the case tumours showed lower VHL protein expression compared to normal kidney tissue (Figure 3F).

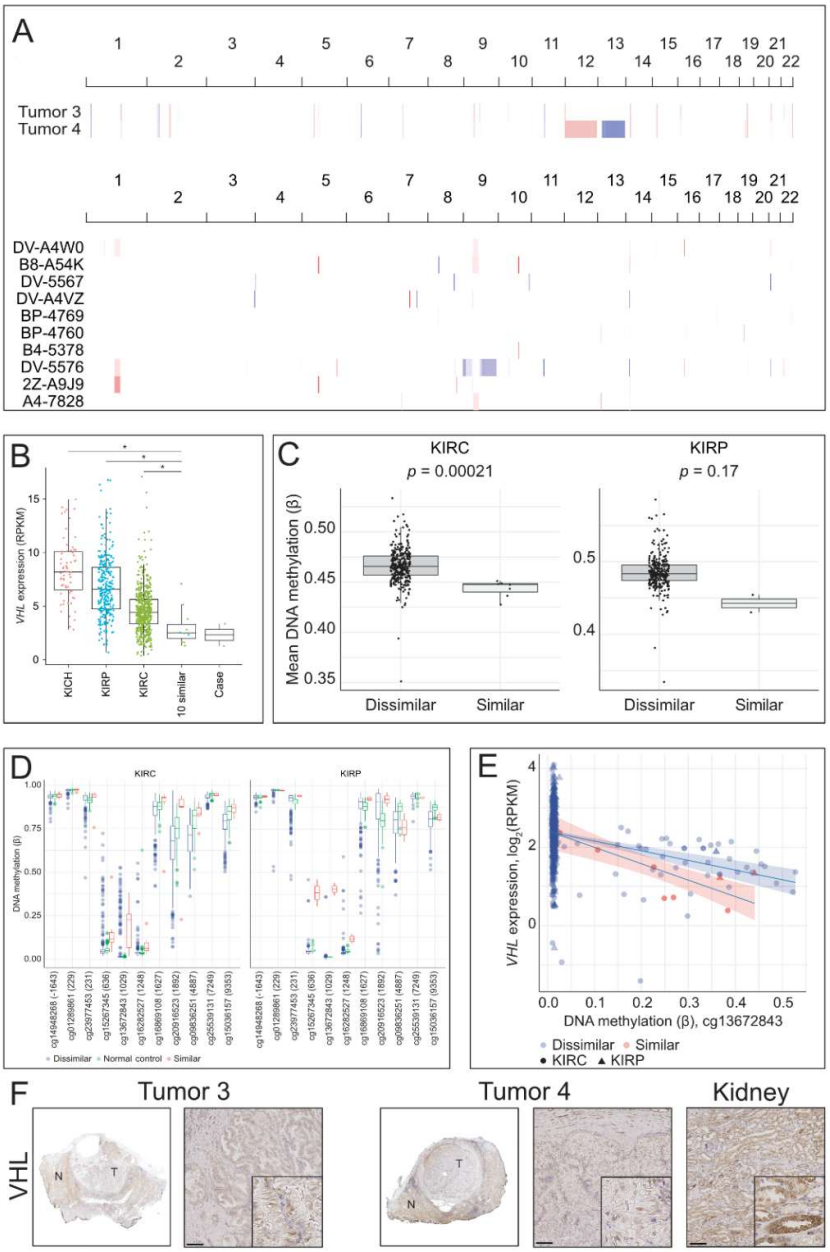

Figure 3. Genomic and histological analysis suggests strong similarities within the identified cluster. (**A**) Somatic copy number profiles of index-case tumours (T3/T4) and the identified 10 similar. No major genomic alterations are present such chromosomal loss or rearrangements (**B**) Transcriptomic analysis of the *VHL* gene with low average expression in the identified subcluster. (**C**) Mean DNA Methylation with low methylation rate among similar cases. (**D**) CpG probes for *VHL* (Illumina Methylation Array) with increased methylation of several important probes compared to clear cell and papillary renal cell carcinoma. (**E**) *VHL* expression correlated against DNA methylation of cg13672843 located at exon 1. Significant decline in *VHL* expression is noted with methylation rate. (**F**) Immunohistochemistry of our case with lower VHL protein expression compared to normal kidney tissue. Scale bar = 200µm. *VHL*, von Hippel-Lindau tumour suppressor gene; *KIRC*, clear cell renal cell carcinoma; *KIRP*, papillary renal cell carcinoma; *KICH*, chromophobe renal cell carcinoma; *N*, normal tissue; *T*, tumour tissue.

 doi:10.20944/preprints202606.1140.v1

3.4. Somatic Mutations and differential expression

One case of the identified 10 similar had a mutation in *MTORC1*. No other mutations were identified for *TSC1*, *TSC2*, *ELOC* or *MTORC1*. In the index case, a nonsense mutation (stop-gain) at L619 of *TSC2* was observed in tumour T3. T4 exhibited a splice site mutation (rs45454192) in the *TSC2* gene, where 33% of the reads did not splice correctly for *TSC2* (Figure 4A). An unusual germline variant of *TSC2* (V223G) was noted in both normal and T3/T4 samples (data not shown). Two different methods, SIFT and PolyPhen, predicted this variant to be deleterious. Complementary IHC for TSC2 (low expression), p-mTOR (low expression, in demarcated parts higher), and pS6K1 (high expression) indicated that loss of function of TSC2 resulted in activation of the mTOR pathway (Figure 4B). Serial sections of the tumours displayed colocalized IHC staining for p-mTOR and pS6K1. Expression analysis of T3 and T4 highlighted low *TSC2* expression. Gene set enrichment analysis of T3 gene expression revealed higher levels of genes involved in mTOR complex 1 signalling relative to T4 (Supplementary Figure S1), and gene set enrichment analysis of the case and the ten similar to MSigDB Hallmark pathways showed higher than average hypoxia and transforming growth factor beta (TGF-β) signalling and lower activity of pathways related to the handling of reactive oxygen species (Supplementary Figure S1).

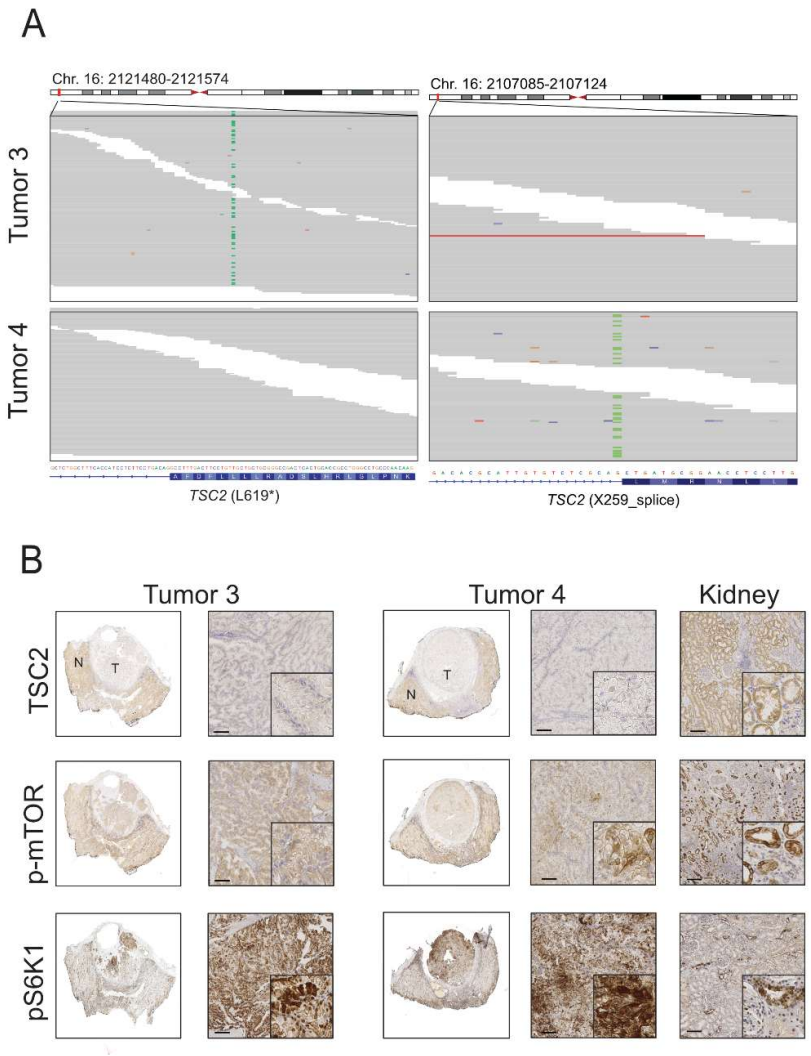

Figure 4. Analysis of mutational status of the index case. (**A**) Subclonal mutations of *TSC2* for tumour 3 and 4. T3 harbours a nonsense mutation (stop-gain) at L619 and T4 a splice site mutation (rs45454192). (**B**)

 doi:10.20944/preprints202606.1140.v1

Immunohistochemistry for TSC2 (low expression), p-mTOR (low expression, in demarcated parts higher) and pS6K1 (high expression) suggests activation of the mTOR pathway in index case. Scale bar = 200 μm. *TSC2,* Tuberous Sclerosis Complex 2; *p-mTOR,* phospho-Mechanistic Target Of Rapamycin Kinase; *pS6K1,* phospho-S6 Kinase 1; *N*, normal tissue; *T,* tumour.

3.5. Clinical and histopathological data from the 10 similar cases

Clinical data for the 10 similar cases in the TCGA data repository and the index case are summarized in Table 1. A comprehensive histological assessment was also performed for all similar cases based on digitalized H/E slides. Immunohistochemistry slides were not available for evaluation. Re-evaluation of the histology revealed substantial interobserver variability (Table 2). Most of the 10 similar cases displayed distinct features of CCPRCT, with mainly clear cell morphology and areas of apical linear distribution of nuclei. In most cases, the fibromuscular stroma was less prominent and focal eosinophilic cells were observed. The remaining cases were histologically similar to the index case, with more prominent stromal component and non-apically oriented nuclei. Thick strands of the fibromuscular bundles were also consistently noted (Appendix 1). However, the diagnostic variability was considerable mainly in distinguishing CCPRTC from RCCFMS. The median age at diagnosis was 61 years, with a male-to-female ratio of 2:1. Available data suggest an indolent course. One case was reported deceased at one year with a T1aNXM0 diagnosis. Follow-up data were unavailable for four cases. Seven of the 10 similar cases had multifocal tumours, according to the pathology report at the time of surgery. Of the 10 similar cases 8 were from patients of African American ethnicity.

Table 1. Clinical overview of index case and the 10 identified similar cases.

Patient	Sex/Age	TNM-stage	Multiple tumours (nr)	Prior malignancy	Year of diagnosis	Ethnicity	5-year OS
Case	M / 50	T1a N0M0	Yes (6)	No	2016	CC	Yes
1	M / 61	T1a NXM0	No	Yes	2012	AA	LTFU
2	M / 63	T1a NXM0	Yes (2)	No	2005	CC	Yes
3	M / 69	T1a NXM0	Yes (3)	Yes	2004	AA	Yes
4	F / 40	T1a N0M0	Yes (11)	Yes	2008	AA	Yes
5	M / 62	T1 NXM0 [a]	No	No	2010	CC	LTFU
6	M / 53	T1a NXMX	Yes (3)	No	2007	AA	LTFU
7	M / 55	T1b NXM0	Yes (9)	No	2008	AA	Yes
8	F / 55	T1a NXM0	Yes (3)	Yes	2008	AA	No
9	M / 77	T1a N0M0	Yes (2)	Yes	2006	AA	Yes
10	F / 74	T1a N0M0	No	No	2011	AA	LTFU

M, male; F, female; TCGA, The Cancer Genome Atlas; Caucasian ; AA, African American; OS, Overall survival; LTFU, lost to follow-up;

[a] T1a or b not specified

 doi:10.20944/preprints202606.1140.v1

Table 2. Primary histology and re-evaluation of the 10 identified similar cases.

Patient	Sex/Age	Primary Classification in TCGA	Flagged in previous marker studies [a]	Histology re-evaluation (MJ)	Histology re-evaluation (ML)	Histology re-evaluation (NM)
1	M / 61	RCC NOS	No	CCPRCT	CCPRCT	RCCFMS
2	M / 63	CCRCC	Yes [1]	RCCFMS	CCRCC	CCRCC
3	M / 69	CCRCC	Yes [2]	CCPRCT	CCPRCT	RCCFMS
4	F / 40	CCRCC	No	RCCFMS	CCRCC	RCCFMS
5	M / 62	CCRCC	Yes [3]	CCPRCT	CCRCC	RCCFMS
6	M / 53	CCRCC	No	RCCFMS	RCCFMS	RCCFMS
7	M / 55	CCRCC	No	CCPRCT	RCCFMS	RCCFMS
8	F / 55	CCRCC	No	CCPRCT	RCCFMS	RCC NOS
9	M / 77	PRCC	No	CCPRCT	CCPRCT	PRCC
10	F / 74	PRCC	Yes [4]	RCCFMS	CCRCC	PRCC

M, male; F, female; TCGA, The Cancer Genome Atlas; RCC, renal cell carcinoma; NOS, not otherwise specified; CCRCC, clear cell renal cell carcinoma; PRCC, papillary renal cell carcinoma; MJ, Martin E Johansson; ML, Martin Lindgren; NM, Niels Marcussen

[a] Chen et.al *Multilevel Genomics-Based Taxonomy of Renal Cell Carcinoma [18]*

[1] "Not Clear Cell or Chromophobe on histopathological re-review"

[2] "Not Clear Cell or Chromophobe on histopathological re-review"

[3] "Suspect molecular profile"

[4] "Not Papillary—Possibly CCRCC"

3.6. Identification and evaluation of potential markers by transcriptomic analysis

Potential markers were identified by differential analysis across genes with high and low expression. Two proteins, COL17A1 and KRT17, were compatible with possible diagnostic markers based on their distinctly high expression and for representing structural proteins suitable as targets for diagnostic antibodies (Figure 5A,B, Supplementary Tables S2 and S3). IHC of the index case demonstrated, consistent with the RNA expression, a general and distinct positive staining for COL17A1 and KRT17. No expression of KRT17 was observed in normal kidneys, whereas COL17A1 was found to be expressed by scattered cells in the collecting ducts. The tissue sections of the tumours displayed a distinct positive signal (Figure 5C). To further examine the expression of COL17A1 and KRT17, TMA: s with 257 CCRCC cases, 68 PRCC cases and 5 cases of recently diagnosed CCPRCT were stained (Table 4). The TMA: s showed no cases of double positive staining for both KRT17 and COL17A1. One case of PRCC and four cases of CCRCC were found to be positive for COL17A1. Of these, sarcomatoid histology were observed in one case and histology comparable to RCCFMS in two cases. For CCPRCT, strong diffuse positive staining of 4/5 (80%) was found for KRT17, and diffuse positive staining of 5/5 (100%) for COL17A1 (Supplementary Table S5).

 doi:10.20944/preprints202606.1140.v1

Table 4. Positive staining pattern for KRT17 and COL17A1.

	No. of cases	KRT17 (%)	COL17A1 (%)
TMA CCRCC	257	1 (< 1) [a]	4 (1.6) [b]
TMA PRCC	68	1 (1.5)	1 (1.5) [c]
CCPRCT	6	5 (83)	6 (100)

TMA, tissue microarray; CCRCC, clear cell renal cell carcinoma; PRCC, papillary renal cell carcinoma; CCPRCT, clear cell papillary renal cell tumor; KRT17, cytokeratin 17; COL17A1, Collagen Type XVII Alpha 1 Chain

[a] Sarcomatoid clear cell renal cell carcinoma

[b] One case with sarcomatoid features. One case compatible with renal cell carcinoma with leiomyomatous stroma.

[c] Histology compatible with renal cell carcinoma with leiomyomatous stroma.

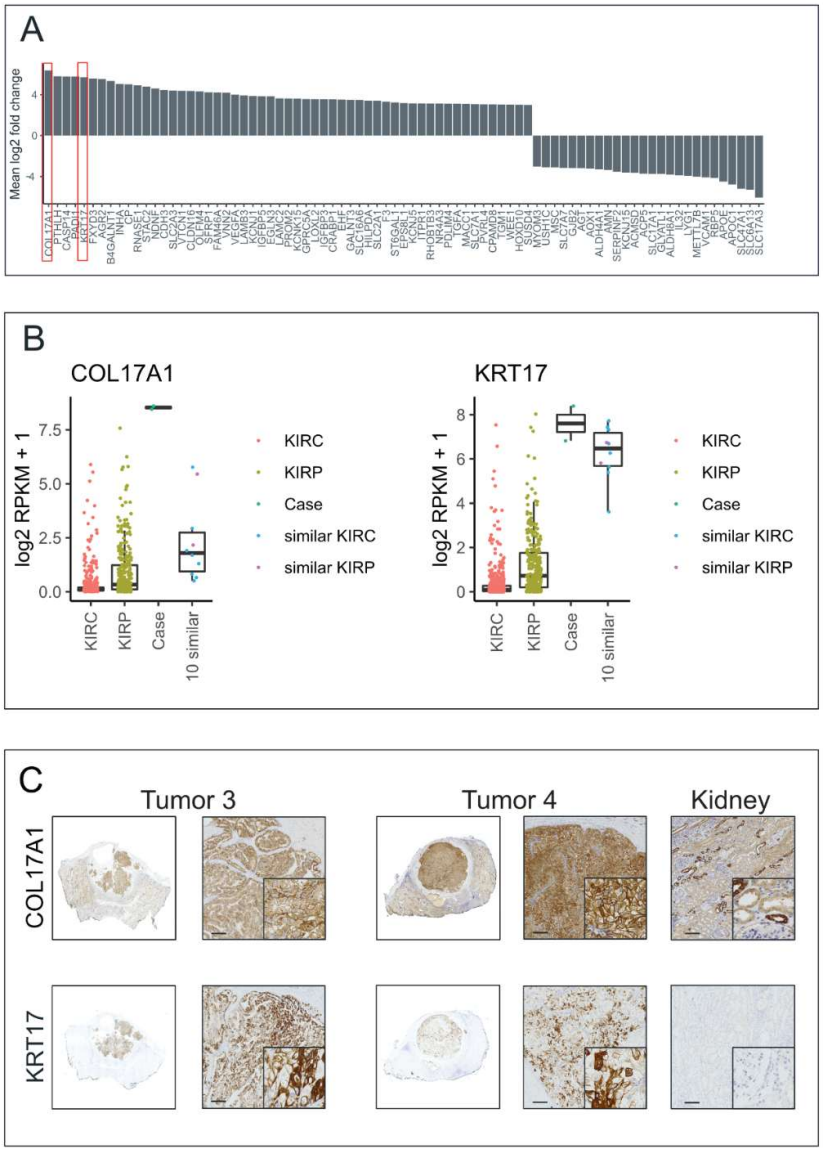

Figure 5. Transcriptional analysis of the index-case and subcluster cases reveals potential markers. (**A**) Expression analysis of the identified subcluster including the index case identifies *KRT17* and *COL17A1* as

 doi:10.20944/preprints202606.1140.v1

possible markers. (**B**) Transcriptional analysis of markers with significantly higher expression compared to clear cell (KIRC) and papillary renal cell carcinoma (KIRP). (**C**) Immunohistochemistry for KRT17 (diffuse high expression in tumours, low in normal kidney) and COL17A1 (diffuse high expression in tumours, high expression in normal kidney proximal tubules). Scale bar = 200µm. *COL17A1*, Collagen Type XVII Alpha 1 Chain; *KRT17*, Cytokeratin 17; *RPKM*, Reads per kilobase per million.

4. Discussion

In this exploratory study, we identified a case of multifocal RCC with a clear cell tubulopapillary growth pattern lacking apically oriented nuclei and with thick fibromyomatous stroma. The case also displayed a "cup-shaped" CAIX positivity and diffuse CK7 positivity. The features were most consistent to the non-established diagnosis of RCCFMS, with resemblance to CCPRCT. By subjecting two tumours to DNA and RNA sequencing and comparing their transcriptional and genomic profiles to 885 RCC cases in the TCGA database, we aimed to identify similar tumours in an unbiased manner. Our analysis suggests a potential biological relationship between at least some cases of RCCFMS and CCPRCT, raising the possibility that these tumours may represent variants of indolent clear cell tumours within the same spectrum although this requires validation.

The recognition of CCPRCT in the 2016 WHO classification was significant, marking the first acknowledgment of an indolent clear cell tumour [5]. Delineation of rare tumour subtypes is not always straightforward. RAT for instance, was initially described as distinct, later to be incorporated into the CCPRCT category [5,33]. RCCFMS in contrast, has been provisionally maintained as a separate entity, on histological grounds, with leiomyomatous stromal bands and absence of the nuclei forming an abluminal picket fence position distinguishing it from CCPRCT [2,14]. Yet stromal components have been questioned as reliable diagnostic criteria, as similar features are also seen in more common RCC types such as CCRCC and PRCC [34,35]. In a cohort of 18 RCCFMS cases, Shah et al. reported molecular alterations involving the TSC/mTOR pathway [10]. In a comparative study by Li et al. 5 patients with TSC/mTOR and 7 patients with TCEB1/ELOC alterations were studied, both with RCCFMS morphology. The clinical characteristics, however, differed substantially, with a mean age of 23 years (range 19–30) and ISUP grade 2–3 in the TSC/mTOR patients, indicating biological variability [36]. These observations support the previous notion that RCCFMS likely represents a heterogeneous entity with similar morphology [37]. Gupta et al. have highlighted the challenges of applying genetic diagnostic criteria in routine pathology. They also propose a reversion from tumour to the previous designation indolent carcinoma, which could broaden the diagnostic criteria for CCPRCT [38]. We concur with this view, particularly in cases of more advanced age, low-grade nuclei, and small tumours.

In this study, clinical data from the identified tumours reported low tumour stage (T1), absence of metastases and a generally indolent course. One of the 10 patients had deceased within five years. This was a patient with T1aNXM0 who died one year after diagnosis. There is no information on the cause of death, but it is unlikely that the cause was disseminated RCC, given the TNM status at diagnosis. The available data suggests that the aggressiveness of tumours in the sub-cluster is low or very low. All cases displayed clear cell morphology, and seven cases showed areas of apically oriented nuclei that would categorize them as CCPRCT, while three had features consistent with RCCFMS. Of note, leiomyomatous strands were observed not only in RCCFMS but also in several CCPRCT cases. The finding of overlapping features support the notion that these tumours are difficult to separate in routine diagnostics.

On the molecular level, the subgroup was characterized by diploid genomes and absence of common driver mutations, in contrast to sporadic CCRCC, where 3p loss and VHL inactivation are hallmarks [39]. RNA-seq did not detect any increase in mTOR activity. A clear cell histology suggests involvement of the VHL/HIF pathway. Downregulation of VHL mRNA was consistently observed, with evidence of hypermethylation at specific CpG sites. Importantly, these findings highlight that epigenetic mechanisms, rather than genetic mutations, can underlie tumour development in this subgroup. Previous studies on epigenetic silencing of *VHL* have specifically pointed towards

 doi:10.20944/preprints202606.1140.v1

cg13672843, which is positioned at the beginning of exon 1 [18,40]. Therefore, we postulate that epigenetic factors cause pseudohypoxic realignment of cellular metabolism, resulting in a clear cell phenotype. Immunohistochemistry for VHL confirmed lower VHL expression than in normal kidney tissue. We propose that epigenetic silencing of *VHL* may contribute to a pseudohypoxic realignment and clear cell phenotype in these tumours.

Positivity for CK7 and diffuse "cup-shaped" CAIX positivity are shared features for RCCFMS and CCPRCT in contrast to the "box-shaped" expression associated with CCRCC. In normal CAIX expressing tissues such as the gall bladder epithelium, intestinal crypts, and efferent ducts of the testis, CAIX is predominantly localized to the basolateral membranes. Cup shaped expression is therefore probably associated with normal intracellular sorting, a feature that is preserved in both CCPRCT and RCCFMS. Therefore, CAIX and CK7 expression may be less suitable in the differential diagnosis of CCPRCT vs. RCCFMS. E-cadherin is also expressed basolateral in the index case, which further strengthens the assumption of a conserved cell sorting apparatus.

The index case displayed strong diffuse CD10 positivity, as well as a lack of apical alignment of nuclei. CD10 positivity has been noted to some extent (2-24%) in previous reports of CCPRCT [41–43]. Two of the identified 10 similar tumours (TCGA-DV-5567 and TCGA-BP-4760) have also previously been highlighted as probable CCPRCT [44].

An unusual germline mutation in TSC2 (V223G) was identified in the index case that was predicted to result in loss of function for the protein. In addition, sub-clonal variation appears to be present, with tumour T3 having a nonsense mutation (stop-gain) at L619 and T4 having a splice site mutation (rs45454192). Considering multifocality and bilateral tumour localization, a hereditary underlying risk factor seems to be present with tumour development possibly caused by a "second hit" in different ways in the two tumours examined. Bilateral tumours are strongly associated with hereditary kidney cancer, without necessarily belonging to any of the known hereditary syndromes [45,46]. A review of the pathology reports for each case showed that 7 of 10 individuals underwent excision of multiple tumours during surgery. Clinical data have also revealed a significant occurrence of other malignancies, albeit without specific details. In CCPRCT, a high incidence of bilateral disease (up to 25%) has been reported [41,47].

In our study, we also observed a high prevalence of African American ethnicity compared to the entire TCGA RCC dataset (72% vs. 13%). Interestingly, several previous studies have reported a substantial increase in the occurrence of CCPRCT among African Americans, further supporting elements of a hereditary component [41,42,48]. A similar distribution of sex and age at diagnosis was common in the identified tumours. Previous malignancies were registered in 5 (50%) of the 10 similar cases. This is an interesting observation; however, whether an increased risk of other malignancies exists in this group cannot be answered in this study.

We raise the possibility that CCPRCT and at least a subgroup of tumour with features of RCCFMS may represent morphological variants within a similar spectrum. Positive markers for this category would be valuable; therefore, we examined the list of differentially expressed genes in the cases. The highly expressed structural proteins COL17A1and KRT17 were selected for further analysis. Unlike most other collagens, COL17A1 is a transmembrane protein. Furthermore, it is part of the multiprotein complex formed by hemidesmosomes that anchor the cell to the basal cell membrane. For instance, basal stem cells of the epidermis are anchored to the basal membrane by COL17A1 [49]. The index case was positive for both KRT17 and COL17A1. We also stained TMA samples containing 257 CCRCC and 68 PRCC tumours. All cases showed negative staining, except for one case of PRCC. An independent cohort of five cases of CCPRCT were stained for KRT17 and COL17A1, and all displayed positivity in most of the tumour tissue.

Three urological pathologists from independent universities re-evaluated the 10 cases based on available H&E histology. A considerable interobserver variability was noted, highlighting the challenges of primary diagnosis. Especially regarding the distinction between RCCFMS, CCRCC and CCPRCT. The identified markers may possibly aid in identifying CCRCC cases from cases with a

 doi:10.20944/preprints202606.1140.v1

potentially more indolent clinical course. This could be of particular importance in diagnosing biopsy material with limited tumour content.

Strengths of this study include DNA- and RNA-seq to a very high depth, which is a key factor in applying comparative sequencing-based analysis [50]. The cluster formation is unsupervised and independent of the included case, and the identified similar tumours share many morphological and clinical traits further supporting their resemblance. However, it is difficult to compare different sequencing platforms. In TCGA, patients from several different centres with different platforms over several years were included. This potential source of analytical error has previously been pointed out [15,51].

This study has several important limitations. First, the analysis is centred on a single index case, and the identification of similar tumours in the TCGA dataset is based on an exploratory, transcriptome-driven approach, which may be sensitive to methodological and batch-related variation. Second, we lack histological material from TCGA tumours for confirmatory immunohistochemistry. Third, clinical follow-up data for several TCGA cases were incomplete, restricting assessment of biological behaviour. Taken together, these limitations indicate that the findings should be interpreted as hypothesis-generating and require validation in larger, prospectively characterized cohorts.

5. Conclusions

We identified a cluster of indolent renal tumours with clear cell morphology from the TCGA database by comparing whole genome sequencing data from an index case with features overlapping CCPRCT and the non-established subtype RCCFMS. The TCGA cluster showed similar clinical characteristics with morphology closely resembling both CCPRCT and RCCFMS. The tumours lacked identifiable driver mutations and exhibited downregulation of VHL, likely mediated by epigenetic silencing. Our findings suggest that CCPRCT could share important molecular and morphological traits with a subset of tumours best described as RCCFMS without major genetic alterations. Our results should be regarded as hypothesis-generating and further studies in larger cohorts are warranted. Importantly KRT17 and COL17A1 emerged as candidate diagnostic markers, that may aid in recognition of this tumour subgroup.

Supplementary Materials: The following supporting information can be downloaded at the website of this paper posted on Preprints.org, Figure S1: Gene set enrichment analysis; Table S1: IHC; Table S2: KIRC vs Case; Table S3: KIRP vs Case; Table S4: TCGA identification; Table S5: CCPRCT staining; Table S6: TCGA abbreviation list.

Author Contributions: Conceptualization, R.J. and M.E.J.; methodology, R.J., Y.A., J.K. and M.E.J.; software, J.K.; validation, R.J., Y.A, J.K. and M.E.J.; formal analysis, R.J., M.L., Y.A., J.K. and M.E.J.; investigation, R.J., M.L., Y.A., N.M, J.K. and M.E.J.; resources, Y.A.; data curation, R.J., Y.A. and J.K.; writing—original draft preparation, R.J., J.K. and M.E.J.; writing—review and editing, R.J., M.L., Y.A., I.J., J.A.N., N.M, J.K. and M.E.J.; visualization, R.J and Y.A..; supervision, J.K and M.E.J; project administration, Y.A and M.E.J.; funding acquisition, R.J. and M.E.J. All authors have read and agreed to the published version of the manuscript.

Funding: This research was funded by: The Swedish Cancer Society (Cancerfonden) grant number 21 1767 Pj 01 H; The Swedish state under the agreement between the Swedish government and the county councils, (ALF); The Assar Gabrielsson Foundation grant number FB23-110; The Research Fund (R&D) at Skaraborg Hospital, Skövde, Sweden; The Healthcare Committee, Region Västra Götaland, Sweden.

Institutional Review Board Statement: The study was conducted in accordance with the Declaration of Helsinki, and approved by the Regional Ethical Review Board of Gothenburg for the use of clinical materials for research purposes including genetic analysis (Dnr: 2019-00905).

Informed Consent Statement: Informed consent was obtained from all subjects involved in the study.

 doi:10.20944/preprints202606.1140.v1

Data Availability Statement: The original contributions presented in this study are included in the article/supplementary material. Further inquiries can be directed to the corresponding author(s).

Acknowledgments: We wish to thank laboratory technician Gülay Altiparmak, for her skilled technical assistance.

Conflicts of Interest: The authors declare no conflicts of interest. The funders had no role in the design of the study; in the collection, analyses, or interpretation of data; in the writing of the manuscript; or in the decision to publish the results.

Abbreviations

The following abbreviations are used in this manuscript:

MDPI	Multidisciplinary Digital Publishing Institute
DOAJ	Directory of open access journals
TLA	Three letter acronym
LD	Linear dichroism
AE1-3	Epithelial Antibody cocktail 1-3
BAM	Binary Alignment Map
CAIX	Carbonic anhydrase IX
CCPRCT	Clear cell papillary renal cell tumour
CCRCC	Clear cell renal cell carcinoma
CD10	Cluster of differentiation 10
CHRCC	Chromophobe renal cell carcinoma
COL17A1	Collagen Type XVII Alpha 1 Chain
COSMIC	Catalogue Of Somatic Mutations In Cancer
CpG	Cytosine-phosfate-Guanine
dbSNP	Single Nucleotide Polymorphism Database
Dnr	Diarie number / registry number
ECAD	E-cadherin
ELOC	Elongin C
EMA	Epithelial membrane antigen
ESP	Exome Sequencing Project
GATK	Genome Analysis Toolkit
GRCh37	Genome Reference Consortium Human Build 37
GSVA	Gene Set Variation Analysis
H&E	Hematoxylin and eosin
IHC	Immunohistochemistry
KRT17 /CK17	Cytokeratin 17
KRT7 / CK7	Cytokeratin 7
ML	Martin Lindström
MJ	Martin E. Johansson
MSigDB	Molecular Signatures Database
MTORC1	mammalian target of rapamycin complex 1
p-mTOR	phospho-Mechanistic Target of Rapamycin Kinase
p-S6K1	phospho-S6 Kinase 1
PRCC	Papillary renal cell carcinoma
RAT	Renal angiomyomatous tumour
RCC	Renal cell carcinoma
RCCFMS	Renal cell carcinoma with prominent fibromyomatous stroma
RJ	Rasmus Jakobsson
RNA	Ribonucleic acid
RPKM	Reads per kilobase per million
SAM	Sequence Alignment Map
TCGA	The Cancer Genome Atlas
TGF-β	Transforming growth factor beta
TMA	Tissue microarray
TSC1	Tuberous Sclerosis Complex 1

 doi:10.20944/preprints202606.1140.v1

TSC2	Tuberous Sclerosis Complex 2
t-SNE	t-distributed stochastic neighbor embedding
UCSC	University of California Santa Cruz
VEP	Variant Effect Predictor
VHL	von Hippel–Lindau tumour suppressor
WGS	Whole genome sequencing
WHO	The World Health Organisation

References

1. Kovacs, G.; Akhtar, M.; Beckwith, B.J.; Bugert, P.; Cooper, C.S.; Delahunt, B.; Eble, J.N.; Fleming, S.; Ljungberg, B.; Medeiros, L.J.; et al. The Heidelberg classification of renal cell tumours. *J Pathol* **1997**, *183*, 131-133, doi:10.1002/(SICI)1096-9896(199710)183:2<131::AID-PATH931>3.0.CO;2-G.
2. Moch, H.; Amin, M.B.; Berney, D.M.; Comperat, E.M.; Gill, A.J.; Hartmann, A.; Menon, S.; Raspollini, M.R.; Rubin, M.A.; Srigley, J.R.; et al. The 2022 World Health Organization Classification of Tumours of the Urinary System and Male Genital Organs-Part A: Renal, Penile, and Testicular Tumours. *European urology* **2022**, *82*, 458-468, doi:10.1016/j.eururo.2022.06.016.
3. Trpkov, K.; Hes, O.; Williamson, S.R.; Adeniran, A.J.; Agaimy, A.; Alaghehbandan, R.; Amin, M.B.; Argani, P.; Chen, Y.B.; Cheng, L.; et al. New developments in existing WHO entities and evolving molecular concepts: The Genitourinary Pathology Society (GUPS) update on renal neoplasia. *Mod Pathol* **2021**, *34*, 1392-1424, doi:10.1038/s41379-021-00779-w.
4. Eble, J.N. Contributions of genetics to the evolution of the diagnostic classification of renal cell neoplasia: a personal perspective. *Pathology* **2021**, *53*, 96-100, doi:10.1016/j.pathol.2020.10.004.
5. Moch, H.; Cubilla, A.L.; Humphrey, P.A.; Reuter, V.E.; Ulbright, T.M. The 2016 WHO Classification of Tumours of the Urinary System and Male Genital Organs-Part A: Renal, Penile, and Testicular Tumours. *European urology* **2016**, *70*, 93-105, doi:10.1016/j.eururo.2016.02.029.
6. Michal, M.; Hes, O.; Havlicek, F. Benign renal angiomyoadenomatous tumor: a previously unreported renal tumor. *Ann Diagn Pathol* **2000**, *4*, 311-315, doi:10.1053/adpa.2000.17890.
7. Adam, J.; Couturier, J.; Molinie, V.; Vieillefond, A.; Sibony, M. Clear-cell papillary renal cell carcinoma: 24 cases of a distinct low-grade renal tumour and a comparative genomic hybridization array study of seven cases. *Histopathology* **2011**, *58*, 1064-1071, doi:10.1111/j.1365-2559.2011.03857.x.
8. Bhatnagar, R.; Alexiev, B.A. Renal-cell carcinomas in end-stage kidneys: a clinicopathological study with emphasis on clear-cell papillary renal-cell carcinoma and acquired cystic kidney disease-associated carcinoma. *Int J Surg Pathol* **2012**, *20*, 19-28, doi:10.1177/1066896911414273.
9. Shah, R.B. Renal Cell Carcinoma With Fibromyomatous Stroma-The Whole Story. *Adv Anat Pathol* **2022**, *29*, 168-177, doi:10.1097/PAP.0000000000000337.
10. Shah, R.B.; Stohr, B.A.; Tu, Z.J.; Gao, Y.; Przybycin, C.G.; Nguyen, J.; Cox, R.M.; Rashid-Kolvear, F.; Weindel, M.D.; Farkas, D.H.; et al. "Renal Cell Carcinoma With Leiomyomatous Stroma" Harbor Somatic Mutations of TSC1, TSC2, MTOR, and/or ELOC (TCEB1): Clinicopathologic and Molecular Characterization of 18 Sporadic Tumors Supports a Distinct Entity. *Am J Surg Pathol* **2020**, *44*, 571-581, doi:10.1097/PAS.0000000000001422.
11. Gupta, S.; McCarthy, M.R.; Tjota, M.Y.; Antic, T.; Cheville, J.C. Metastatic renal cell carcinoma with fibromyomatous stroma associated with tuberous sclerosis or MTOR, TSC1/TSC2-Mutations: A Series of 4 cases and a review of the literature. *Hum Pathol* **2024**, *153*, 105680, doi:10.1016/j.humpath.2024.105680.
12. Zhu, Y.; Fang, M.; Wang, S. ELOC(TCEB1)-mutated renal cell carcinoma: a case report and clinicopathological analysis. *Front Oncol* **2025**, *15*, 1703364, doi:10.3389/fonc.2025.1703364.
13. Williamson, S.R.; Gupta, N.S.; Eble, J.N.; Rogers, C.G.; Michalowski, S.; Zhang, S.; Wang, M.; Grignon, D.J.; Cheng, L. Clear Cell Renal Cell Carcinoma With Borderline Features of Clear Cell Papillary Renal Cell Carcinoma: Combined Morphologic, Immunohistochemical, and Cytogenetic Analysis. *Am J Surg Pathol* **2015**, *39*, 1502-1510, doi:10.1097/PAS.0000000000000514.
14. Trpkov, K.; Williamson, S.R.; Gill, A.J.; Adeniran, A.J.; Agaimy, A.; Alaghehbandan, R.; Amin, M.B.; Argani, P.; Chen, Y.B.; Cheng, L.; et al. Novel, emerging and provisional renal entities: The Genitourinary

 doi:10.20944/preprints202606.1140.v1

Pathology Society (GUPS) update on renal neoplasia. *Mod Pathol* **2021**, *34*, 1167-1184, doi:10.1038/s41379-021-00737-6.

15. Cancer Genome Atlas Research, N. Comprehensive molecular characterization of clear cell renal cell carcinoma. *Nature* **2013**, *499*, 43-49, doi:10.1038/nature12222.
16. Cancer Genome Atlas Research, N.; Linehan, W.M.; Spellman, P.T.; Ricketts, C.J.; Creighton, C.J.; Fei, S.S.; Davis, C.; Wheeler, D.A.; Murray, B.A.; Schmidt, L.; et al. Comprehensive Molecular Characterization of Papillary Renal-Cell Carcinoma. *N Engl J Med* **2016**, *374*, 135-145, doi:10.1056/NEJMoa1505917.
17. Davis, C.F.; Ricketts, C.J.; Wang, M.; Yang, L.; Cherniack, A.D.; Shen, H.; Buhay, C.; Kang, H.; Kim, S.C.; Fahey, C.C.; et al. The somatic genomic landscape of chromophobe renal cell carcinoma. *Cancer Cell* **2014**, *26*, 319-330, doi:10.1016/j.ccr.2014.07.014.
18. Chen, F.; Zhang, Y.; Senbabaoglu, Y.; Ciriello, G.; Yang, L.; Reznik, E.; Shuch, B.; Micevic, G.; De Velasco, G.; Shinbrot, E.; et al. Multilevel Genomics-Based Taxonomy of Renal Cell Carcinoma. *Cell Rep* **2016**, *14*, 2476-2489, doi:10.1016/j.celrep.2016.02.024.
19. Kim, D.; Langmead, B.; Salzberg, S.L. HISAT: a fast spliced aligner with low memory requirements. *Nat Methods* **2015**, *12*, 357-360, doi:10.1038/nmeth.3317.
20. Anders, S.; Pyl, P.T.; Huber, W. HTSeq--a Python framework to work with high-throughput sequencing data. *Bioinformatics* **2015**, *31*, 166-169, doi:10.1093/bioinformatics/btu638.
21. Bagge, R.O.; Demir, A.; Karlsson, J.; Alaei-Mahabadi, B.; Einarsdottir, B.O.; Jespersen, H.; Lindberg, M.F.; Muth, A.; Nilsson, L.M.; Persson, M.; et al. Mutational Signature and Transcriptomic Classification Analyses as the Decisive Diagnostic Tools for a Cancer of Unknown Primary. *JCO Precis Oncol* **2018**, *2*, doi:10.1200/PO.18.00002.
22. Van Der Maaten, L.; Hinton, G. Visualizing data using t-SNE. *Journal of Machine Learning Research* **2008**, *9*, 2579-2625.
23. Liberzon, A.; Birger, C.; Thorvaldsdottir, H.; Ghandi, M.; Mesirov, J.P.; Tamayo, P. The Molecular Signatures Database (MSigDB) hallmark gene set collection. *Cell Syst* **2015**, *1*, 417-425, doi:10.1016/j.cels.2015.12.004.
24. Korotkevich, G.; Sukhov, V.; Budin, N.; Shpak, B.; Artyomov, M.N.; Sergushichev, A. Fast gene set enrichment analysis. *bioRxiv* **2021**, 060012, doi:10.1101/060012.
25. Li, H.; Durbin, R. Fast and accurate short read alignment with Burrows-Wheeler transform. *Bioinformatics* **2009**, *25*, 1754-1760, doi:10.1093/bioinformatics/btp324.
26. McKenna, A.; Hanna, M.; Banks, E.; Sivachenko, A.; Cibulskis, K.; Kernytsky, A.; Garimella, K.; Altshuler, D.; Gabriel, S.; Daly, M.; et al. The Genome Analysis Toolkit: a MapReduce framework for analyzing next-generation DNA sequencing data. *Genome Res* **2010**, *20*, 1297-1303, doi:10.1101/gr.107524.110.
27. Benjamin, D.; Sato, T.; Cibulskis, K.; Getz, G.; Stewart, C.; Lichtenstein, L. Calling Somatic SNVs and Indels with Mutect2. *bioRxiv* **2019**, 861054, doi:10.1101/861054.
28. Karczewski, K.J.; Francioli, L.C.; Tiao, G.; Cummings, B.B.; Alföldi, J.; Wang, Q.; Collins, R.L.; Laricchia, K.M.; Ganna, A.; Birnbaum, D.P.; et al. The mutational constraint spectrum quantified from variation in 141,456 humans. *Nature* **2020**, *581*, 434-443, doi:10.1038/s41586-020-2308-7.
29. Adzhubei, I.A.; Schmidt, S.; Peshkin, L.; Ramensky, V.E.; Gerasimova, A.; Bork, P.; Kondrashov, A.S.; Sunyaev, S.R. A method and server for predicting damaging missense mutations. *Nat Methods* **2010**, *7*, 248-249, doi:10.1038/nmeth0410-248.
30. Sim, N.L.; Kumar, P.; Hu, J.; Henikoff, S.; Schneider, G.; Ng, P.C. SIFT web server: predicting effects of amino acid substitutions on proteins. *Nucleic Acids Res* **2012**, *40*, W452-457, doi:10.1093/nar/gks539.
31. Ricketts, C.J.; De Cubas, A.A.; Fan, H.; Smith, C.C.; Lang, M.; Reznik, E.; Bowlby, R.; Gibb, E.A.; Akbani, R.; Beroukhim, R.; et al. The Cancer Genome Atlas Comprehensive Molecular Characterization of Renal Cell Carcinoma. *Cell Rep* **2018**, *23*, 313-326.e315, doi:10.1016/j.celrep.2018.03.075.
32. Gutman, D.A.; Khalilia, M.; Lee, S.; Nalisnik, M.; Mullen, Z.; Beezley, J.; Chittajallu, D.R.; Manthey, D.; Cooper, L.A.D. The Digital Slide Archive: A Software Platform for Management, Integration, and Analysis of Histology for Cancer Research. *Cancer Res* **2017**, *77*, e75-e78, doi:10.1158/0008-5472.Can-17-0629.

 doi:10.20944/preprints202606.1140.v1

33. Michal, M.; Hes, O.; Nemcova, J.; Sima, R.; Kuroda, N.; Bulimbasic, S.; Franco, M.; Sakaida, N.; Danis, D.; Kazakov, D.V.; et al. Renal angiomyoadenomatous tumor: morphologic, immunohistochemical, and molecular genetic study of a distinct entity. *Virchows Arch* **2009**, *454*, 89-99, doi:10.1007/s00428-008-0697-3.
34. Petersson, F.; Branzovsky, J.; Martinek, P.; Korabecna, M.; Kruslin, B.; Hora, M.; Peckova, K.; Bauleth, K.; Pivovarcikova, K.; Michal, M.; et al. The leiomyomatous stroma in renal cell carcinomas is polyclonal and not part of the neoplastic process. *Virchows Arch* **2014**, *465*, 89-96, doi:10.1007/s00428-014-1591-9.
35. Hes, O.; Comperat, E.M.; Rioux-Leclercq, N. Clear cell papillary renal cell carcinoma, renal angiomyoadenomatous tumor, and renal cell carcinoma with leiomyomatous stroma relationship of 3 types of renal tumors: a review. *Ann Diagn Pathol* **2016**, *21*, 59-64, doi:10.1016/j.anndiagpath.2015.11.003.
36. Li, H.; Argani, P.; Halper-Stromberg, E.; Lotan, T.L.; Merino, M.J.; Reuter, V.E.; Matoso, A. Positive GPNMB Immunostaining Differentiates Renal Cell Carcinoma With Fibromyomatous Stroma Associated With TSC1/2/MTOR Alterations From Others. *Am J Surg Pathol* **2023**, *47*, 1267-1273, doi:10.1097/PAS.0000000000002117.
37. Trpkov, K.; Hes, O. New and emerging renal entities: a perspective post-WHO 2016 classification. *Histopathology* **2019**, *74*, 31-59, doi:10.1111/his.13727.
38. Gupta, S.; Dasari, S.; Sharma, V.; Atwell, T.D.; Sivasankaran, G.; Smoley, S.A.; Hardcastle, J.J.; Lohse, C.M.; Tekin, B.; Jimenez, R.E.; et al. Metastatic clear cell papillary renal cell 'tumour'. *Histopathology* **2024**, *84*, 905-909, doi:10.1111/his.15123.
39. Hsieh, J.J.; Le, V.H.; Oyama, T.; Ricketts, C.J.; Ho, T.H.; Cheng, E.H. Chromosome 3p Loss-Orchestrated VHL, HIF, and Epigenetic Deregulation in Clear Cell Renal Cell Carcinoma. *J Clin Oncol* **2018**, *36*, Jco2018792549, doi:10.1200/jco.2018.79.2549.
40. Zhang, Y.; Yang, L.; Kucherlapati, M.; Chen, F.; Hadjipanayis, A.; Pantazi, A.; Bristow, C.A.; Lee, E.A.; Mahadeshwar, H.S.; Tang, J.; et al. A Pan-Cancer Compendium of Genes Deregulated by Somatic Genomic Rearrangement across More Than 1,400 Cases. *Cell Rep* **2018**, *24*, 515-527, doi:10.1016/j.celrep.2018.06.025.
41. Weng, S.; DiNatale, R.G.; Silagy, A.; Mano, R.; Attalla, K.; Kashani, M.; Weiss, K.; Benfante, N.E.; Winer, A.G.; Coleman, J.A.; et al. The Clinicopathologic and Molecular Landscape of Clear Cell Papillary Renal Cell Carcinoma: Implications in Diagnosis and Management. *European urology* **2021**, *79*, 468-477, doi:10.1016/j.eururo.2020.09.027.
42. Alexiev, B.A.; Drachenberg, C.B. Clear cell papillary renal cell carcinoma: Incidence, morphological features, immunohistochemical profile, and biologic behavior: A single institution study. *Pathol Res Pract* **2014**, *210*, 234-241, doi:10.1016/j.prp.2013.12.009.
43. Aron, M.; Chang, E.; Herrera, L.; Hes, O.; Hirsch, M.S.; Comperat, E.; Camparo, P.; Rao, P.; Picken, M.; Michal, M.; et al. Clear cell-papillary renal cell carcinoma of the kidney not associated with end-stage renal disease: clinicopathologic correlation with expanded immunophenotypic and molecular characterization of a large cohort with emphasis on relationship with renal angiomyoadenomatous tumor. *Am J Surg Pathol* **2015**, *39*, 873-888, doi:10.1097/pas.0000000000000446.
44. Xu, J.; Reznik, E.; Lee, H.J.; Gundem, G.; Jonsson, P.; Sarungbam, J.; Bialik, A.; Sanchez-Vega, F.; Creighton, C.J.; Hoekstra, J.; et al. Abnormal oxidative metabolism in a quiet genomic background underlies clear cell papillary renal cell carcinoma. *Elife* **2019**, *8*, doi:10.7554/eLife.38986.
45. Jakobsson, R.G.; Nasic, S.; Bratt, O.; Johansson, M.E.; Grenabo Bergdahl, A. Family History and Risk of Renal Cell Carcinoma: A National Multiregister Case-Control Study. *J Urol* **2024**, *211*, 71-79, doi:10.1097/ju.0000000000003765.
46. Ljungberg, B.; Albiges, L.; Abu-Ghanem, Y.; Bedke, J.; Capitanio, U.; Dabestani, S.; Fernandez-Pello, S.; Giles, R.H.; Hofmann, F.; Hora, M.; et al. European Association of Urology Guidelines on Renal Cell Carcinoma: The 2022 Update. *European urology* **2022**, *82*, 399-410, doi:10.1016/j.eururo.2022.03.006.
47. Williamson, S.R. Clear cell papillary renal cell carcinoma: an update after 15 years. *Pathology* **2021**, *53*, 109-119, doi:10.1016/j.pathol.2020.10.002.
48. Wang, K.; Zarzour, J.; Rais-Bahrami, S.; Gordetsky, J. Clear Cell Papillary Renal Cell Carcinoma: New Clinical and Imaging Characteristics. *Urology* **2017**, *103*, 136-141, doi:10.1016/j.urology.2016.12.002.

 doi:10.20944/preprints202606.1140.v1

49. Thangavelu, P.U.; Krenacs, T.; Dray, E.; Duijf, P.H. In epithelial cancers, aberrant COL17A1 promoter methylation predicts its misexpression and increased invasion. *Clin Epigenetics* **2016**, *8*, 120, doi:10.1186/s13148-016-0290-6.
50. Sims, D.; Sudbery, I.; Ilott, N.E.; Heger, A.; Ponting, C.P. Sequencing depth and coverage: key considerations in genomic analyses. *Nat Rev Genet* **2014**, *15*, 121-132, doi:10.1038/nrg3642.
51. Whalley, J.P.; Buchhalter, I.; Rheinbay, E.; Raine, K.M.; Stobbe, M.D.; Kleinheinz, K.; Werner, J.; Beltran, S.; Gut, M.; Hübschmann, D.; et al. Framework for quality assessment of whole genome cancer sequences. *Nat Commun* **2020**, *11*, 5040, doi:10.1038/s41467-020-18688-y.